IP2016 / 4th International Workshop on Induced Polarization

Mapping and characterization of Induced Polarization in airborne TEM data from central East Greenland – application of a Self-Organizing Map procedure

Anaïs Brethes
GEUS, LTU
Øster Volgade 10,
1350 København K - Denmark
aib@geus.dk

Thorkild M. Rasmussen
Luleå University of Technology (LTU)
971 87 Luleå,
Sweden
thorkild.maack.rasmussen@ltu.se

Pierpaolo Guarnieri
GEUS
Øster Volgade 10,
1350 København K - Denmark
pgua@geus.dk

Tobias Bauer
LTU
971 87 Luleå,
Sweden
tobias.bauer@ltu.se

SUMMARY

Induced Polarization (IP) effects were observed in airborne Time Domain EM (TEM) data acquired in central East Greenland in the context of exploration for disseminated sulphides in a sedimentary basin. Some of the IP anomalies were targeted by drilling which revealed the absence of mineralization. In order to understand the possible causes of the IP effects we first identified them in the TEM data. IP indicators were extracted from the shape of the transient curves at every measurement location and were analysed by using a Self-Organizing Map (SOM) procedure. Results from K-mean clustering of the SOM are visualized on a geographical map showing the transient curves' characteristics. Some of the clusters are clearly correlated with the geology whereas others merely reflect recordings below the noise level. In order to interpret the cause of the IP anomalies the airborne TEM data were inverted for the Cole-Cole parameters.

Key words: Induced Polarization, Self-Organizing Map (SOM), Airborne Time-Domain EM, Cole-Cole parameters

INTRODUCTION

A high-resolution dual moment, i.e. Low Moment (LM) and High Moment (HM) airborne time-domain electromagnetic survey was conducted along the eastern margin of the Jameson Land basin in central East Greenland to explore for base metals. The survey area comprises crystalline basement to the East and layered Early Triassic to Jurassic sediments to the West. The layers are dipping a few degrees towards West. The Triassic sequence is 1 to 2km thick and mostly of continental origin. The fluviatile Early Triassic arkoses and conglomerates, the lower Middle Triassic grey limestone and black shale beds and overlying gypsiferous sandstones and mudstones are known to host disseminated sulphides (Harpøth et al., 1986). Sulphide mineralization was the target of an airborne TEM survey acquired with a SkyTEM system over an area of 550km^2. N-S oriented lines were flown with an average terrain clearance of 30m and a separation of 300m while E-W oriented tie-lines were flown with 4km separation. Additional lines were flown over 3 areas of particular interest with different orientation and a separation of 150m. The data were processed and inverted by SkyTEM Aps.

The conductivity models showed some conductive layers as well as IP effects in the data. IP effects in TEM data reflect the relaxation of polarized charges in the ground which can be good indicators of the presence of metallic particles. Some of these locations were drilled during the following field season but unfortunately did not reveal the presence of mineralization. The aim of this study is therefore to understand the possible causes of these IP effects. The remote location of the area prevents the data to be affected by cultural noise such as power lines, fences, etc. The electrical charge accumulation in the ground can be related to the presence of sulphides, oxides or graphite or to the presence of clays or fibrous minerals. Permafrost may also cause IP effects and is then expected to be associated with a highly resistive subsurface.

In order to spatially locate the areas where IP effects occur in the TEM data and compare them with the geology, the shape of the transient curve was analysed. IP effects can be indicated in the transients by:

- the presence of negative values;
- a very fast or very slow rate of decay of the positive part of the soundings (Smith and Klein, 1996).

Several characteristics of the transient curves (IP indicators) of the SkyTEM survey were extracted and analysed by using the Self-Organizing Map (SOM) technique. This is a type of neural network algorithm developed by Kohonen (2001) for analysis of multivariate data. The basic idea of SOM is to provide a method for easy visualizing of multi-dimensional data. The SOM may be viewed as a two-dimensional grid onto which multi-dimensional input data are projected or mapped from a multi-dimensional space (the space dimension is equal to the number of input variables) containing all the geographically distributed data characteristics from the transient curves. Input data that are similar or close to each other, irrespectively of geographic location, are mapped to the same or adjacent position in the SOM. A standard K-mean clustering procedure on the SOM grid is used to perform yet another simplification for easy visualization. Data that belongs to a particular cluster in the SOM data space can afterward be mapped into a geographical map. The SiroSOM software (Fraser and Dickson, 2007) was used for the SOM analysis. Once IP were identified and located, Cole-Cole parameters were recovered from the airborne TEM data in specific locations using the program AarhusInv developed by the hydrogeophysics group of Aarhus university (Auken et al., 2014).

SELF ORGANIZING MAP AND SPATIAL ANALYSIS OF THE IP EFFECTS

LM and HM data were respectively recorded over 20 and 21 gates from 12 to 1220µs and from 119 to 14686µs. The transients were analysed at every 10th measurement location along the flight lines for which 15 parameters (IP indicators) were calculated: (1) the sum of all negative values, (2) the sum of negative values in the most early local minimum, (3) the first negative value, (4) the gate of the first negative value, (5) the minimum value, (6) the gate of the minimum value, (7) the number of gates of consecutive negative values, (8) the maximum descending slope in the negative part, (9) the gate of the maximum descending slope in the negative part, (10) the maximum ascending slope in the negative part, (11) the gate of the maximum ascending slope in the negative part, (12) the maximum descending slope in the entire curve, (13) the gate of the maximum descending slope in the entire curve, (14) the maximum ascending slope in the entire curve, and (15) the gate of the maximum ascending slope in the entire curve.

Two examples of HM response curves are shown in Figure 1, which illustrates some of the characteristics of the survey data. The example from line L303101 (Figure 1a) has a very well-defined local minimum with 9 consecutive negative values in early gates. This is considered a clear indication of IP effects in the data. The example from Line 301901 (Figure 1a, b) has 3 consecutive negative values at the latest gates. A small local minimum with positive values is observed prior to the negative values. The data from the late gates from Line 301901 are close to or below the noise level. However, inspection of adjacent sample locations show a similar pattern, but it is difficult to exclude that systematic noise is causing the observed pattern.

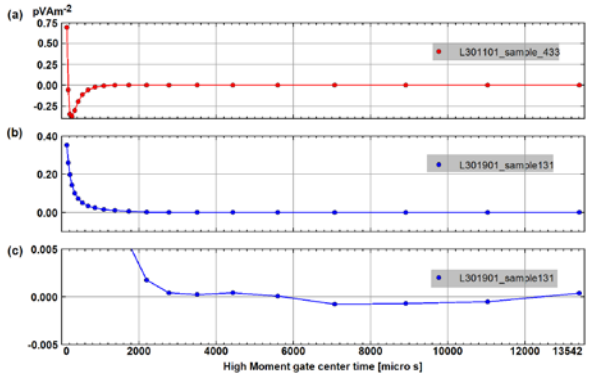

Figure 1. Examples of response curves from HM data. (a) data from L301101 with clear indication of IP effects; (b) data from Line L301901 showing possible but uncertain indications of IP, (c) similar as in (b) but different ordinate values.

For this study, HM data and LM data are analysed separately but they could easily also be analysed jointly. Prior to the SOM analysis of the response curve characteristics, the data were smoothed laterally using a running mean filter applied respectively over 345 points and 65 points to the HM and LM data. The running mean filtering was applied for random noise reduction. Each data type is furthermore normalized by their standard deviation for floating point number and by the range for integers. SOM grid cell sizes of 66x60 and 64x58 were used for the HM and LM data respectively. Figure 2 shows the 14 K-mean clusters of the SOM (grid) obtained from the analysis of the 15 dimensional HM data. SOM component maps corresponding to each of the 15 HM IP indicators are shown in Figure 3, which provides easy visualization of data correlations. The link between individual clusters and IP indicators can be seen by comparing similar grid locations in the maps shown in Figures 2 and 3. The corresponding geographical location of data within each cluster is shown in Figure 4 on the geological map.

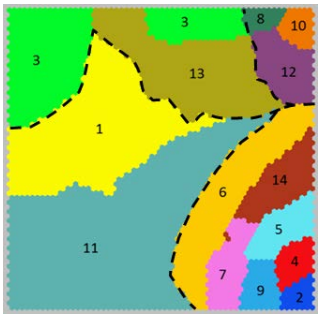

Figure 2. The fourteen K-mean clusters in SOM data space (66x60 grid cells) based on HM data. The dashed lines separate four clusters' groups based on the response curve pattern they represent and on the geological units they are correlated with.

A possible cause to the IP effects in this arctic area is permafrost. In this case, IP indicators would be expected over the whole survey area whereas it seems that they are localised to specific places that are discussed in the following paragraphs.

Inspection of Figures 2 and 3 shows that the clusters numbered 3, 8, 10, 12 and 13 have their first negative value of the transient curve at a very late gate. This may be explained by the signal being below noise level in the late gates as illustrated in Figure 1bc. They show very steep descending slope in the very first gates. Three of these clusters (8, 10 and 12) are located in alluvial fans close to the sea and along river beds where high conductivity is indicated in the surface layers. They are therefore considered not associated with IP. On the contrary, the clusters 2, 4, 5, 9 and 14 represent transient curves with the minimum values of the sum of negatives and their first negative and minimum values appear in the first time gates. They furthermore show negative values for at least 13 gates and may be considered as strong IP effects.

Some clusters (1 and 11 in HM data and 1, 4, 7, 8 and 13 in LM data [not shown]) are associated almost exclusively with areas where crystalline basement is outcropping (see Figure 4). The transient curves corresponding to the clusters from LM data start with negative values and then quickly become positive with oscillating behaviour within the noise level in the late gates. In the HM data the transient curves do not have significant negative values. Cluster 11 represent response curves that have the same pattern than in the LM data and cluster number 1 represents transient curves starting with positive but low values which pass below zero about 8 time gates later. We do not discuss these further in this study.

The remaining clusters which present stronger IP indicators appear to be concentrated in several areas. In the northwestern part of the survey area (see Figure 4a and b), the IP indicators in the HM data reveal a N-S elongated patch of almost

symmetrically distributed clusters (from west to east: clusters 6, 14, 5, 4, 5, 14 and 6). These clusters occur over outcropping Upper Triassic sediments and all describe the same transient curve pattern. However, the most negative sum of negatives, minimum value and first negative value are located in the central part of the patch and increase towards the sides. The minimum and first negative values appear in the earliest time gates and negative values are observed for 12 to 15 consecutive gates. The IP effect in this area is significant and stronger along the N-S elongated central part. This symmetry is less clear in the LM data which show quickly decaying transient curves that pass in the negative values in the late time gates. These elements suggest that the IP source body is elongated in a N-S direction.

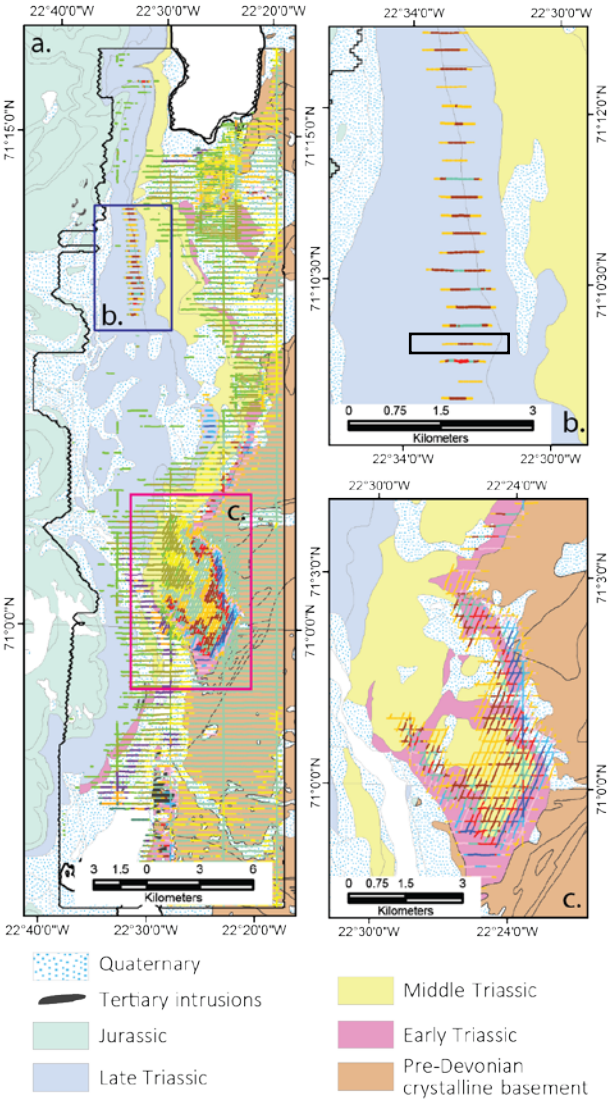

Figure 4. IP indicators plotted with their respective cluster's colour defined from the SOM analysis of the HM TEM data (see Figure 2 for the clusters colour symbols). They are plotted over the simplified geology of the study area. The dark line represents the coverage of the SkyTEM survey and the blue and pink rectangles locate the Figures 4b, and c on which only clusters associated with strong IP effects are displayed. The rectangle on Figure 4b locates the data that are inverted in Figure 5.

In the central part of the survey area (see Figure 4a and c), the clusters are clearly correlated with the outcropping geology both in the LM and HM data. The area where the upper part of Middle Triassic sediments is outcropping is correlated with the clusters 6 and 14 in the HM data. They describe a transient curve which reaches negative values in relatively early time gates and stay in the negative part. Clusters 5, 4, 2, 9, 7 and 6 have the same transient curve shape starting in the negative part. However the clusters 4 and 2 which are correlated with the location of the uppermost part of the Early Triassic formation show curves with the steepest ascending slopes and the most negative sum of negative value. The clusters 7 and 6 are correlated with the transition between the outcropping Early Triassic sediments and the basement and show insignificant IP indicators compared to where Middle and Early Triassic sediments are outcropping in this area. In the same area the clusters in the LM data represent transient curves that all have the same pattern where Early and Middle Triassic sediments outcrop. However, the maximum decaying slope and earliest negative values reached are correlated with areas where the upper Lower Triassic and lower Middle Triassic sediments are outcropping. These elements indicate that the IP effects are correlated with lithological units in the upper part of Early Triassic sediments and lower Middle Triassic sediments that have been described to host base-metal sulphides (Harpøth et al., 1986).

INVERSION FOR COLE-COLE PARAMETERS

To further characterize the possible sources of IP that affect the airborne TEM data we inverted them using AarhusInv to recover their spectral content in terms of resistivity and of Cole-Cole parameters (Pelton et al., 1978). We present results from inversion of a subset of a flight line (see location on Figure 4b) with strong IP effects. The conceptual model used for the inversion presented here contains 4 layers. The noise ascribed to the data is defined as a linear function with slope -0.5 in a logarithmic presentation of data as function of gate centre time. The noise level at 1 ms is defined a $2.5 \cdot 10^{-12}$ T/s. An error floor of 3% is furthermore applied in the noise characterisation. The data entering the inversion are normalised by peak dipole moment and receiver area.

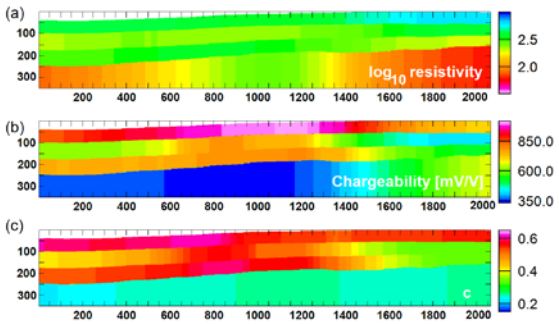

Figure 5. Model obtained from inversion of data from Line 104801 (data are shown in Figure 6)

Figure 5 shows the model and Figure 6 shows the corresponding measured data and model response. The general trend of the measured data is reproduced by the model responses. The highest chargeability values of 900mV/V are confined to the first 150 m in the central part of the section. It is correlated with high frequency constant c values (0.4 - 0.6) and resistivities are relatively low (300 Ωm). As IP effects due

to permafrost would influence the entire area and also show high resistivity values, we reject this possibility for this case. However, at this stage of the modelling it is difficult to discriminate other possible sources of IP effects as the presence of clays or disseminated sulphides.

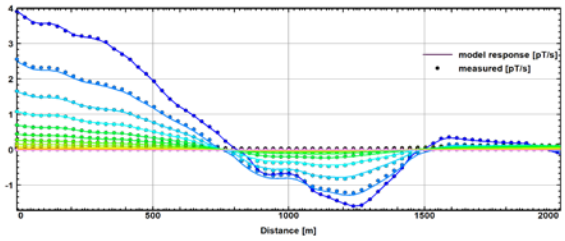

Figure 6. Measured HM data and model responses for the model in Figure 5. Measured data are shown by coloured circles and model responses are shown by corresponding solid lines.

CONCLUSIONS

The SOM analysis of the IP indicators extracted from the transient curves of LM and HM data is a very easy way to visualize the spatial distribution of the IP effects characteristics. Several areas affected by IP effects were described in terms of spatial distribution allowing correlations with the geology. We exclude permafrost as source of the IP effect. The inversion of the TEM data for the Cole-Cole parameters for a selected area was not conclusive with respect to the actual cause of the observed strong IP effect. The inversion however allowed to spatially define the IP source bodies. To complete the study, we will model the complex resistivity measurements from the drillcore samples of this area in order to recover the Cole-Cole parameters and compare them to the modelled IP parameters in the airborne TEM data.

REFERENCES

Auken, E., Christiansen, A.V., Kirkegaard, C., Fiandaca, G., Schamper, C., Behroozmand, A.A., Binley, A., Nielsen, E., Effersø, F., Christensen, N.B., Sørensen, K., Foged, N., Vignoli, G., 2014, An overview of a highly versatile forward and stable inverse algorithm for airborne, ground-based and borehole electromagnetic and electric data: Exploration Geophysics, 46, 223–235.

Fraser, S.J., and Dickson, B.L., 2007, A New Method for Data Integration and Integrated Data Interpretation: Self-Organising Maps: Fifth Decennial International Conference on Mineral Exploration, Toronto, Proceedings of Exploration 07, 907-910.

Harpøth, O., Pedersen, J.L., Schønwandt, H.K., Thomassen, B., 1986, The mineral occurrences of central East Greenland: Meddelelser om Gronland Geoscience 17.

Kohonen, T, 2001, Self-Organizing Maps Third Extended Edition: Springer Series in Information Sciences, vol. 30.

Pelton, W.H., Ward, S.H., Hallof, P.G., Sill, W.R., Nelson, P.H., 1978, Mineral Discrimination and Removal of Inductive Coupling with Multifrequency IP: Geophysics, 43, 588–609.

Smith, R.S., Klein, J., 1996, A special circumstance of airborne induced-polarization measurements: Geophysics, 61, 66 –73.

ACKNOWLEDGEMENTS

This work was conducted as a part of “Crustal Structure and Mineral Deposit Systems: 3D-modelling of base metal mineralization in Jameson Land” (CRUSMID-3D) project, funded by NordMin - A Nordic Network of Expertise for a Sustainable Mining and Mineral Industry

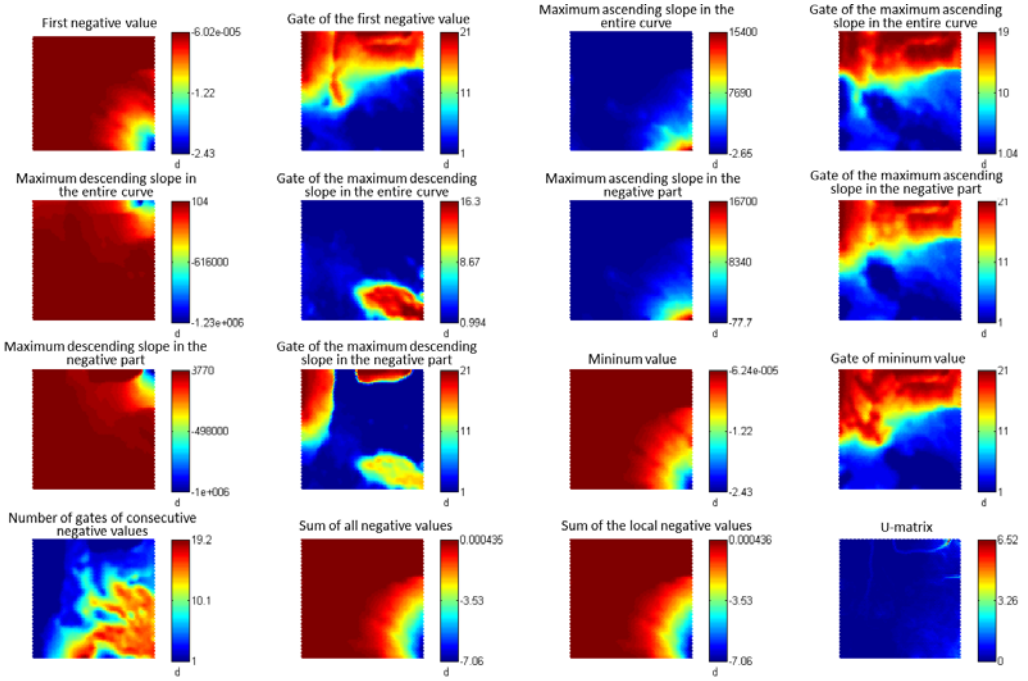

Figure 3. Component maps corresponding to each IP indicator in SOM data space. Similar data are associated with a common best matching unit (BMU) vector and the distance relation between BMUs for a particular grid location and the surrounding BMUs are visualized in the U-matrix by using a colour scale. In the present case, the clustering range is small.